Available online at www.scholarsresearchlibrary.com

Scholars Research Library

Der Pharmacia Lettre, 2016, 8 (15):46-56
(http://scholarsresearchlibrary.com/archive.html)

ISSN 0975-5071
USA CODEN: DPLEB4

Docking Based *De novo* Design of Few Tolcapone Derivatives as Catechol-o-Methyl Transferase (Comt) Inhibitors

Subhadip Ball[1], Subhasis Banerjee[2]* and Amrita Choudhury[3]

[1& 2]Department of Pharmaceutical Chemistry, Gupta College of Technological Sciences, Ashram More, G.T Road, Asansol-713301, Bardhamann, West Bengal, India
[3]Department of Pharmaceutical Chemistry, Jadavpur University, Kolkata, West Bengal 700032

ABSTRACT

Catechol-O-methyl tranferase (COMT; E.C.2.1.1.6) is widely distributed enzyme in nature that plays an essential role in the metabolism of catechol neurotransmitters and catechol linked foreign entities. As L-DOPA, a key medicine in Parkinsonism is being catabolised by COMT, this justified the interest in developing improved COMT inhibitors as significant adjunct to L-DOPA therapy. Although tolcapone have gained considerable attention in bringing therapeutic benefit, yet owing to its fatal hepatotoxic potential entacapone and certain other drug came into existence. The scope for further betterment prompted us to design a series of 48 compounds based on the molecular skeleton of tolcapone have been developed conventionally. In the process of ensuring their drug ability, computational ligand docking methodology, AutoDock 4.0, based on genetic algorithm was employed. Binding mode analysis between docked compounds and the protein were analyzed using ADT (version 1.5.4). The best docking result can be considered to be the conformation which is in the close proximity to the active site along with low (docked) energy. Compounds SB10, SB11, SB31 and SB33 have been found to meet both the stated criteria, thereby chosen to be potent.

Keywords: Parkinsonism, COMT, Tolcapone, Autodock

INTRODUCTION

The emergence of developing antiparkinsonian drugs, trigger the drug discovery process to unveil the topological description of drug target at molecular level. The influence of catechol-O-methyl transferase (COMT) in aggravating the condition of Parkinsonism cannot be ignored. The interest in COMT was rekindled in the late 1980s when the potent and selective second-generation COMT inhibitors were developed [1, 2] and very soon the structures of the two isoforms of COMT and the gene were characterized and COMT polypeptide cDNAs were cloned [3-5]. COMT plays a crucial role in the extracellular metabolism of dopamine and norepinephrine both in the periphery and the central nervous system. COMT-mediated metabolism of levodopa in the periphery influences brain dopamine levels, while the product of central COMT-mediated dopamine metabolism, 3-methoxytyramine, can affect movement via interaction with Trace Amine-Associated Receptor 1 [6]. Nitrocatechols, such as Tolcapone, Entacapone, Nitecapone are so called reversible inhibitors of COMT [7]. These inhibitors have been developed to improve the pharmacokinetics of levodopa and is used as an adjunct to combined levodopa and aromatic amino acid decarboxylase (AADC) inhibitor therapy essential for improved levodopa delivery to the brain [8]. Present research aims at improving biochemistry and molecular biology of COMT and on the pharmacology and clinical efficacy of

the new selective and relative nontoxic COMT inhibitors. *In silico* approaches that describe binding mode of ligands within the active sites of the target and subsequently it is with the scoring functions that further helps in identifying and optimizing lead compounds. Up till now, several COMT inhibitors have found their usefulness in enhancing the therapeutic efficacy of 1 line antiparkinsonian drugs, and this process has been aided by elucidation of several crystallographic structures of COMT. Earlier crystal structure of COMT, PDB entry; 1H1D [9] complexed with cosubstrate SAM and a novel inhibitor BIA shows the atomic interactions between the important residues at the active site and the inhibitor (figure 1).

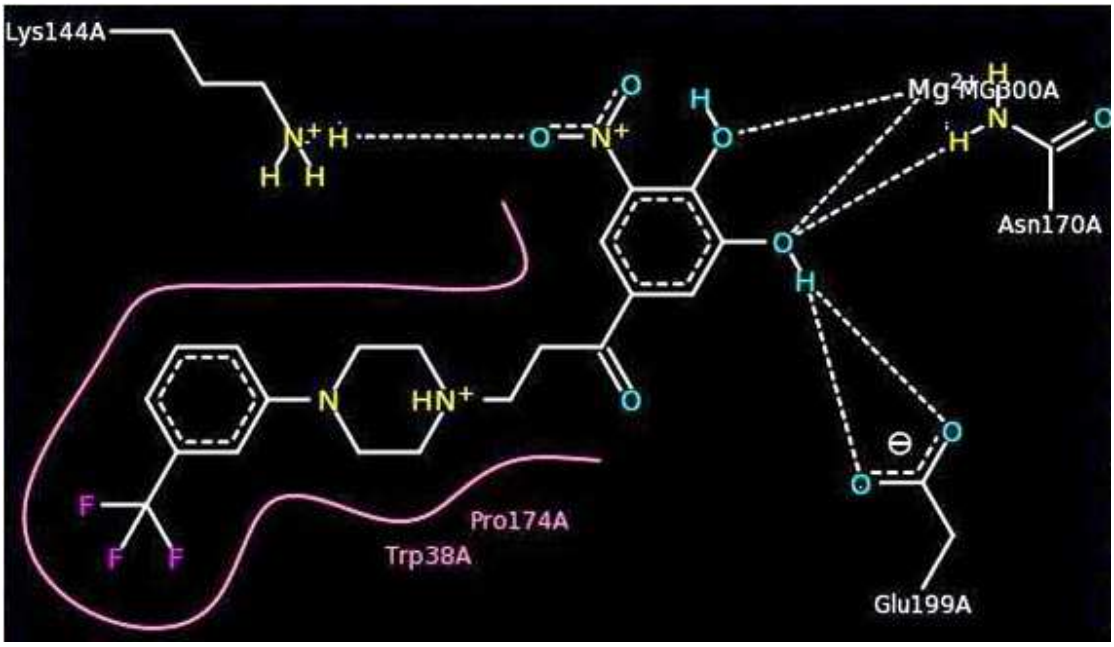

Fig. 1 Active site composition and interaction pattern of BIA, co-crystallized ligand of Catechol-O-methyl transferase (PDB ID: 1H1D)

Computational methods amalgamated with ever rising number of protein structures shift the research paradigm towards macromolecule based drug design, driven by binding mode analysis aided by molecular docking has drawn a considerable attention in drug discovery [10, 11]. Molecular-docking methodologies ultimately seek to predict the best mode by which a given compound will place itself within the binding site of a macromolecule. Docking, as a result, usually involves two independent steps: (1) positioning the ligands in orientations and conformations and (2) the scoring of the ligand's pose such that the ranking typically is an arbitrary reflection of how well a ligand is expected to bind to its complementary residues within the binding sites of the receptor. The re-emergence of such *in-silico*-based screening methods is of practical importance for lead-compound generation in drug discovery. The Docking output has now been proved essential tools that enable computational chemists to rapidly screen large small molecules library and thereby identify promising candidate compounds for further experimental processing. All sampling methods are guided by a function that evaluates the fitness between the protein and ligand. A rigorous search algorithm would exhaustively elucidate all possible binding modes between ligand and receptor. Autodock 4.0 uses GA as a global optimizer combined with energy minimization as a local search method [12]. Our present study aims at developing novel COMT inhibitors considering the molecular framework as 5-nitro catechol of the native ligand. The principles of bio-isosterism have been successfully employed to generate catecholic congeners.

MATERIALS AND METHODS

***COMT modeling*:**

The enzyme model was developed by using AutoDock Tools- 1.5.4 and MGL Tools-1.5.4 packages (The Scripps Research Institute, Molecular Graphics Laboratory, 10550 North Torrey Pines Road, CA, 92037) running on Linux FEDORA 8.0. Initially the 3D crystal structure of catechol-O-methyltransferase; PDB code 1H1D was procured from Brookhaven protein data bank (PDB; http: //www.rcsb. org/pdb) and displayed in python molecular viewer. The nonbonded oxygen atoms of waters, present in the crystal structure were removed. After assigning the bond

orders, missing hydrogen atoms were added, then the partial atomic charges was calculated using

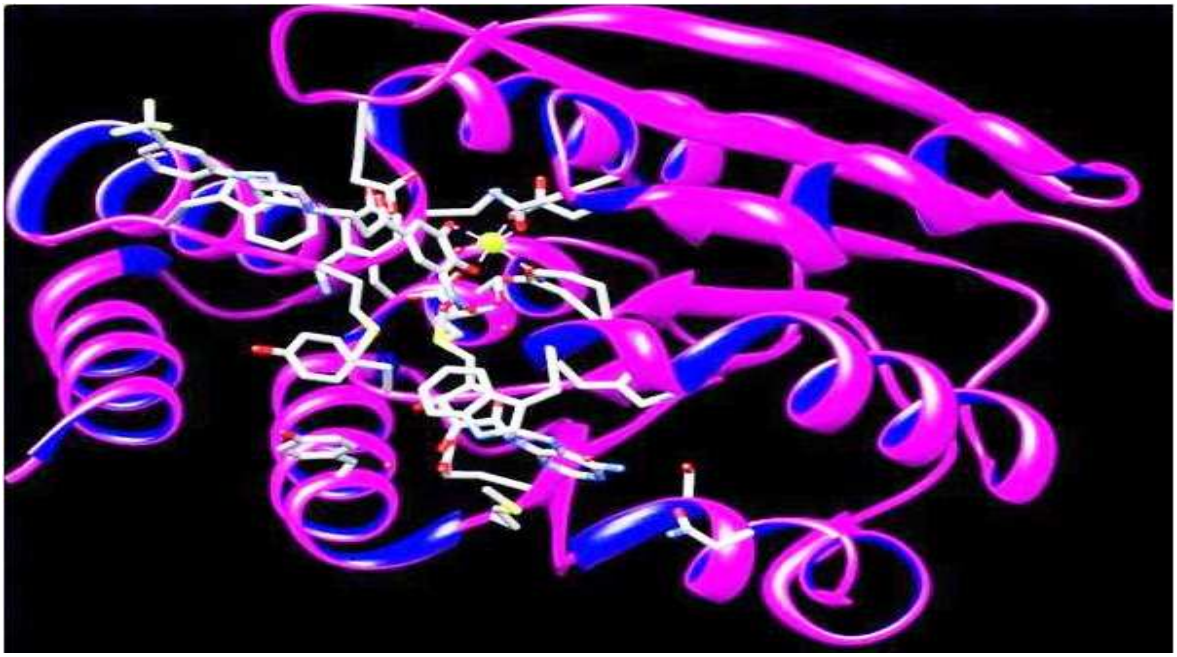

Fig. 2 3D crystal structure of Catechol-O-methyltransferase (PDB ID: 1H1D)

Gasteiger–Marsili method [13]. Kollman [14] united atom charges were assigned, non-polar hydrogens were merged, and rotatable bonds were assigned, keeping all the amide bonds as non-rotatable. The receptor file was converted to pdbqt format, which is pdb plus ‘‘q’’ charges and ‘‘t’’ AutoDock type. (To confirm the AutoDock types, polar hydrogens should be present, whereas nonpolar hydrogens and lone pair should be merged, each atom should be assigned Gasteiger partial charges).

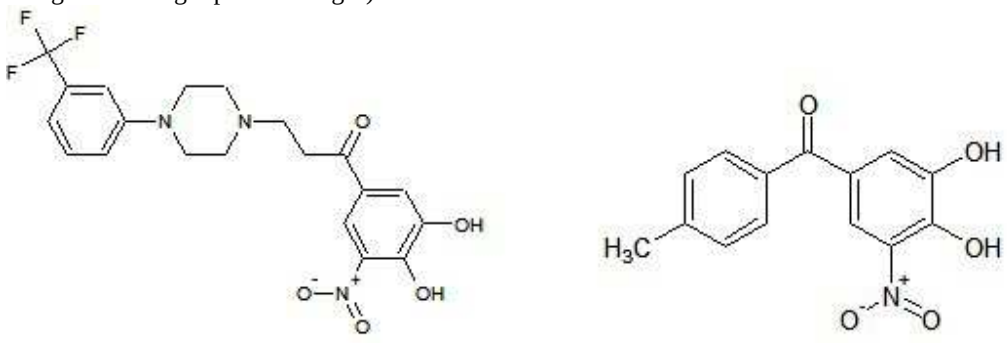

Fig. 3 2D structure of Co crystallized ligand of COMT (BIA335) and Tolcapone

***Validation of the docking protocol in Autodock*:**

The most useful method of evaluating the accuracy of a docking procedure is to determine how closely the least energy conformation predicted by the scoring function resembles an experimental binding mode. In the present study, the docking of BIA 335 which was extracted previously from 1H1D receptor complex into the active site was performed to test the reliability and reproducibility of the docking protocol for our study. We found a significant interaction between the localization of the inhibitor BIA335 upon docking and from the crystal structure. The root mean square deviations (RMSD) between the predicted conformation and the observed X-ray crystallographic conformation of compound BIA 335 equaled 1.70 Å (<3Å) by Autodock. This indicated the reliability of the docking method in reproducing the experimentally observed binding mode for COMT.

***Ligand receptor modeling*:**
Ligand structures were drawn and optimized using PRODRG [15] online server and saved in PDB format. Autodock requires that ligands got partial atomic charges and Autodock atom types for each atom; it also requires an explanation for the rotatable bonds in the ligand. Input molecules files for an Autodock experiments must ensure to the set of atom types supported by it. Torsional degree of freedom (TORSDOF) is used in calculating the change in the free energy caused by the loss of torsional degree of freedom upon binding. In the Autodock 4.0 force field, the TORSDOF value for a ligand is the total number of rotatable bonds in the ligand. This number does not iclude bonds in rings, bonds to leaf atoms, amide bonds, and guanidinium bonds.

***Molecular docking studies*:**
AutoGrid 4.0 [16] was introduced to pre-calculate grid maps of interaction energies of various atom types in all dockings, a grid map with 126*126*126 points, a grid spacing of 0.900 Å (roughly half of the length of a carbon–carbon single bond) were used, and the maps were centered on the macromolecule. In an AutoGrid procedure, the protein is embedded in a 3D grid and a probe atom is placed at each grid point. The energy of interaction of this single atom with the protein is assigned to the grid point. An affinity grid is studied for each type of atoms in the substrate, typically carbon, nitrogen, oxygen, and hydrogens as well as grid of electrostatic potential using a point charge of +1 as the probe [17, 18]. Autodock 4.0 [19, 20] uses these interaction maps to generate ensemble of low energy conformations. It uses a scoring function based on AMBER force field, and estimates the free energy of binding of a ligand to its target. For each ligand atom types, the interaction energy between the ligand atom and the receptor is calculated for the entire binding site which is being judged through a grid. Since a grid map represents the interaction energy as a function of the coordinates, their visual inspection may reveal the potential unsaturated hydrogen acceptors or donors or unfavorable overlaps between the ligand and the receptor. Out of three different search algorithms offered by AutoDock 4.0, the Lamarckian Genetic algorithm (LGA) based on the optimization algorithm was used, since preliminary experiments using other two (Simulated annealing and genetic algorithm) showed that they are less efficient, utilizes Lamarckian notation that an adaptations of an individual to its environment can be inherited by its offspring. For all dockings, 100 independent runs with step sizes of 0.2 Å for translations and 5 Å for orientations and torsions, an initial population of random individuals with a population size of 150 individuals, a maximum number of 2.5*10 energy evaluations, maximum number of generations of 27,000, an elitism value of 1, and a number of active torsion of 5 were used. AutoDock Tools along with AutoDock 4.0 and Auto-Grid 4.0 was used to generate both grid and docking parameter files (i.e., gpf and.dpf files) respectively.

RESULTS AND DISCUSSION

The computational output of LGA docking experiments of COMT inhibitors using AutoDock 4.0 and AutoGrid 4.0 are summarized in Table 1. For each docking operation, the conformer lying within the proximal vicinity of active site was chosen from 100 runs. The central processing unit for a single docking experiment took 80-100 min, on a 2.0 GHz AMD Quad-Core machine with 4.00 GB of RAM and Linux (FEDORA 2008) operating system. In order to evaluate accuracy of docking, binding energy and numbers in cluster was used. Compound SB31 had shown promising binding energy which is even superior to both the co-crystallized ligand as well as the reference standard, tolcapone. The chemical structures of all the 48 compounds are shown in the Figure 4 Modeling and docking analysis revealed the nature of the active site and some key interactions that enabled the binding of tolcapone derivatives to the active site. All the compounds were designed considering the pharmacophoric features of tolcapone, i.e; the essential electronegative group as catecholic hydroxyl, two aromatic moieties, preferentially phenyl and a linker as carbonyl group. The design was mostly centered within the domain of bioisosteric modification. Prior introducing each and every compound into the study, synthetic feasibility has been taken into consideration. The pattern of modification of linker moiety from carbonyl to thiocarbonyl has been adopted from the making of irreversible anticholineesterase. The prototypical structure thus developed assumes the following shape:

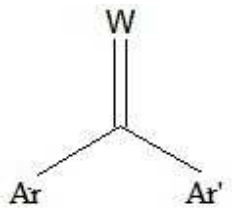

Fig. 4 Basic molecular skeleton of compound SB1-SB46

Table No. 1 Predicted Computational details of compounds considered for the study

Compound code /Confor-mer No	W	Ar	Ar´	Distance (Å)	Binding Energy	Inhibition constant(KI)	Docking rank
SB1/4	O	*p*-anilino	3,4-dihydroxy-5-nitro-phenyl	11.97	-3.16	4.79	09
SB2/24	O	*p*-chlorophenyl	3,4-dihydroxy-5-nitro-phenyl	14.10	-2.73	9.94	15
SB3/3	O	*p*-tolyl	5-nitro-salicyl	14.96	-4.12	954.65	02
SB4/31	O	6-methylpyridyl	5-amino-3,4-dihydroxyphenyl	12.93	-1.36	101.57	42
SB5/47	O	6-aminopyridyl	5-amino-3,4-dihydroxyphenyl	10.27	-0.98	191.58	43
SB6/40	O	6-chloropyridyl	5-amino-3,4-dihydroxyphenyl	11.56	-1.62	65.41	37
SB7/45	O	6-methylpyridyl	5-aminosalicyl	3.53	-1.60	67.66	38
SB8/42	O	6-methylpyridyl	3,4-dihydroxy-5-nitro-phenyl	14.92	-1.75	51.89	35
SB9/42	O	6-aminopyridyl	3,4-dihydroxy-5-nitro-phenyl	16.86	-1.66	62.01	36
SB10/19	S	*p*-tolyl	3,4-dihydroxy-5-nitro-phenyl	9.28	-3.10	5.34	10
SB11/9	O	*p*-tolyl	3-amino-4-hydroxy-5-nitrophenyl	9.55	-3.33	3.61	07
SB12/15	O	*p*-tolyl	4-hydroxy-3-methylamino-5-nitrophenyl	11.00	-3.59	2.35	05
SB13/37	O	*p*-tolyl	3-hydroxyethyl-4hydroxy-5-nitrophenyl	7.51	-2.20	24.57	22
SB14/28	O	*p*-tolyl	3,4-dihydroxy-5-methoxyphenyl	7.06	-2.13	27.37	24
SB15/38	O	*p*-tolyl	3-amino-4-hydroxy-5-methoxyphenyl	10.63	-1.97	35.88	30
SB16/43	O	*p*-tolyl	4-hydroxy-3-methylamino-5-methoxyphenyl	11.63	-2.18	25.14	23
SB17/15	O	*p*-tolyl	3-hydroxyethyl-4-hydroxy-5-methoxyphenyl	4.18	-2.74	9.82	14
SB18/36	O	*p*-bromophenyl	3,4-dihydroxy-5-nitro-phenyl	7.56	-2.42	16.90	20
SB19/40	O	*p*-toludinyl	o-hydroxyphenyl	4.83	-1.77	50.03	34
SB20/11	O	*p*-toludinyl	2-bromo-6-hydroxyphenyl	6.25	-2.87	7.89	12
SB21/50	O	*p*-toludinyl	4-bromo-6-hydroxyphenyl	8.96	-1.62	64.65	37
SB22/1	S	*p*-anilino	3,4-dihydroxy-5-nitro-phenyl	14.27	-4.14	924.11	01
SB23/39	S	*p*-chlorophenyl	3,4-dihydroxy-5-nitro-phenyl	12.79	-2.08	30.05	25
SB24/46	S	*p*-bromophenyl	3,4-dihydroxy-5-nitro-phenyl	3.73	-2.01	33.70	27
SB25/37	S	*p*-fluorophenyl	3,4-dihydroxy-5-nitro-phenyl	7.00	-1.99	34.61	28
SB26/11	S	*p*-tolyl	4-hydroxy-3-methylamino-5-nitrophenyl	11.00	-3.85	1.50	04
SB27/34	S	*p*-anilino	4-hydroxy-3-methylamino-5-nitrophenyl	9.39	-2.49	14.84	18
SB28/41	S	*p*-chlorophenyl	4-hydroxy-3-methylamino-5-nitrophenyl	8.39	-2.32	19.91	21
SB29/22	S	*p*-bromophenyl	4-hydroxy-3-methylamino-5-nitrophenyl	11.54	-2.91	7.32	11
SB30/47	S	*p*-fluorophenyl	4-hydroxy-3-methylamino-5-nitrophenyl	9.58	-1.92	39.01	31
SB31/2	S	*p*-tolyl	3-amino-4-hydroxy-5-nitrophenyl	9.72	-4.05	1.07	03
SB32/47	S	*p*-anilino	3-amino-4-hydroxy-5-nitrophenyl	9.58	-1.41	92.05	40
SB33/17	S	*p*-bromophenyl	3-amino-4-hydroxy-5-nitrophenyl	8.71	-3.10	5.35	10
SB34/47	S	*p*-chlorophenyl	3-amino-4-hydroxy-5-nitrophenyl	11.99	-1.54	73.84	39
SB35/40	S	*p*-iodophenyl	3-amino-4-hydroxy-5-nitrophenyl	10.83	-1.99	34.49	28
SB36/24	S	*p*-tolyl	3-amino-4-hydroxy-5-methoxyphenyl	12.32	-2.44	16.38	19
SB37/3	S	*p*-anilino	3-amino-4-hydroxy-5-methoxyphenyl	5.05	-2.77	9.37	13
SB38/35	S	*p*-chlorophenyl	3-amino-4-hydroxy-5-methoxyphenyl	9.66	-1.82	46.68	33
SB39/46	S	*p*-bromophenyl	3-amino-4-hydroxy-5-methoxyphenyl	11.97	-1.62	64.85	37
SB40/34	S	*p*-fluorophenyl	3-amino-4-hydroxy-5-methoxyphenyl	8.05	-1.87	42.41	32
SB41/22	O	thienyl	3-amino-4-hydroxy-5-nitrophenyl	11.29	-2.58	12.79	17
SB42/47	O	thienyl	3-methylamino-4-hydroxy-5-nitrophenyl	11.88	-1.98	35.14	29
SB43/38	O	thienyl	3,4-dihydroxy-5-nitrophenyl	10.70	-2.59	12.60	16
SB44/14	S	thienyl	3-methylamino-4-hydroxy-5-nitrophenyl	10.36	-3.47	2.86	06
SB45/47	S	5-chlorothienyl	3-methylamino-4-hydroxy-5-nitrophenyl	8.60	-1.87	42.39	32
SB46/50	S	thienyl	3-amino-4-hydroxy-5-nitrophenyl	15.70	-1.37	99.05	41
Co-crystallised ligand: BIA335/17				8.52	-3.18	31.71	08
Reference standard: Tolcapone/24				4.53	-2.82	4.68	26

All the 48 compounds including the reference as tolcapone were screened, the docking interactions of (3,4dihydroxy-5-nitrophenyl)(4-methylphenyl)methanethione(SB10), (3-amino-4-hydroxy-5-nitrophenyl) (4methyl phenyl) methanone(SB11), (3-amino-4-hydroxy-5-nitrophenyl)(4-methylphenyl)methanethione (SB31), (3-amino-4-hydroxy-5-nitrophenyl)(4-bromophenyl)methanethione(SB33)with the active site residues, like Trp38, Lys144, Asn170, Pro174, Glu199 appeared to be in proximity and explains the higher selectivity to the enzyme. Since Mg300 plays a significant role in context to interaction profile, the poses which have been considered for interaction were indeed very close to the ion. It further confirms the possibilities of ionic interaction. Apart from other interaction the compounds have exhibited favorable hydrogen bonding interaction as well. Docking poses and binding interactions of all the potent inhibitors and tolcapone are shown in Figures 5, 6, 7, 8 and 9.

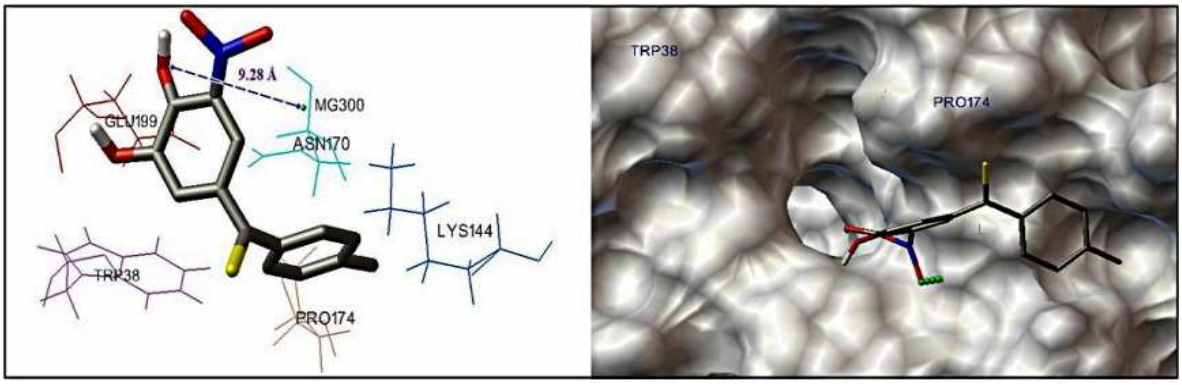

Fig. 5 Stereo and molecular surface view of the docking predicted pose and interaction of compound SB10 within the active site of 1H1D

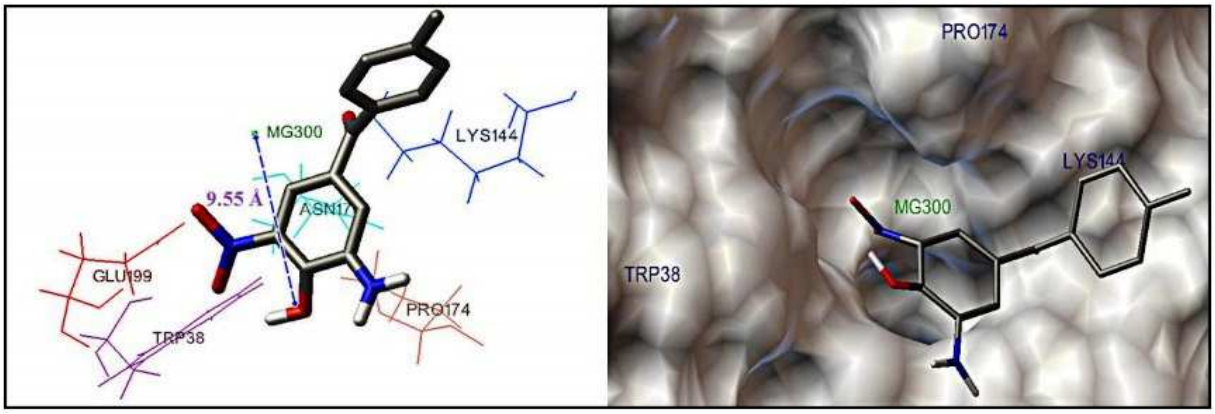

Fig. 6 Stereo and molecular surface view of the docking predicted pose and interaction of compound SB11 within the active site of 1H1D

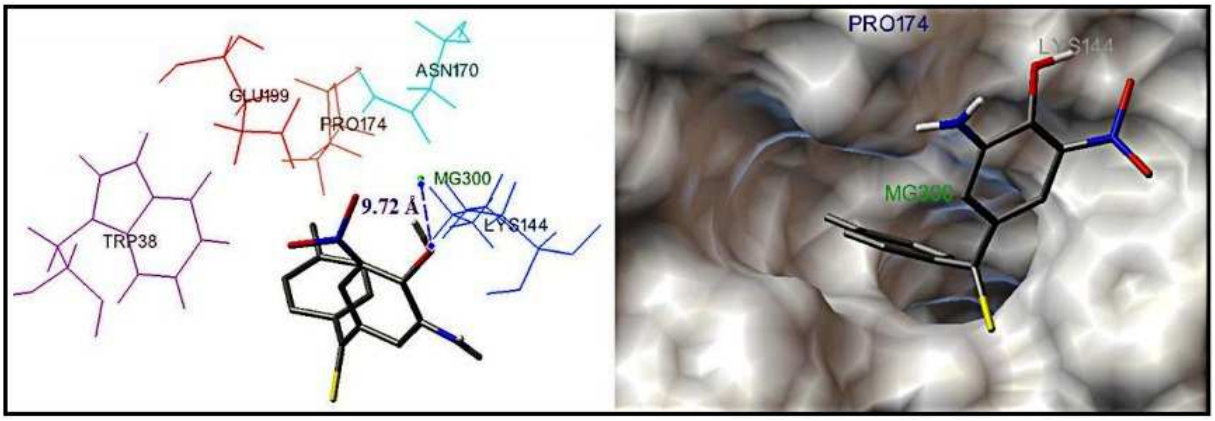

Fig. 7 Stereo and molecular surface view of the docking predicted pose and interaction of compound SB31 within the active site of 1H1D

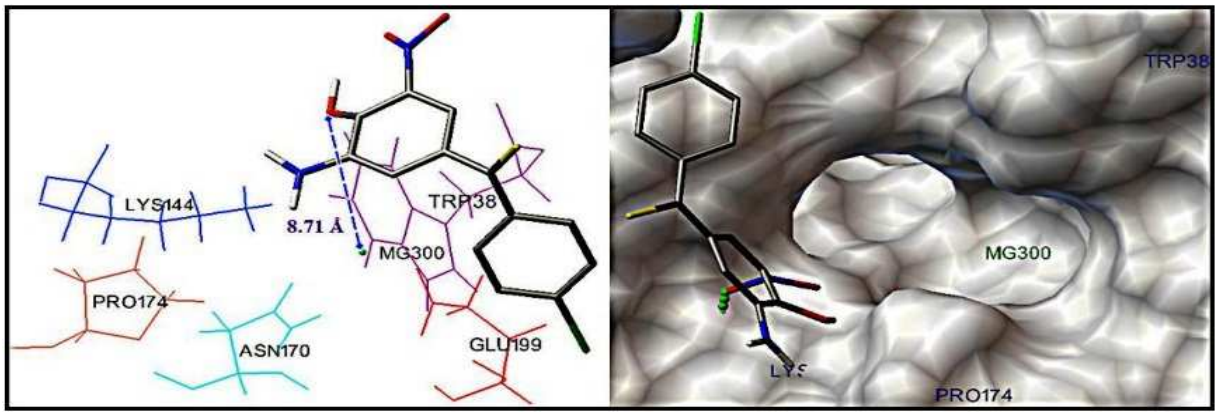

Fig. 8 Stereo and molecular surface view of the docking predicted pose and interaction of compound SB33 within the active site of 1H1D

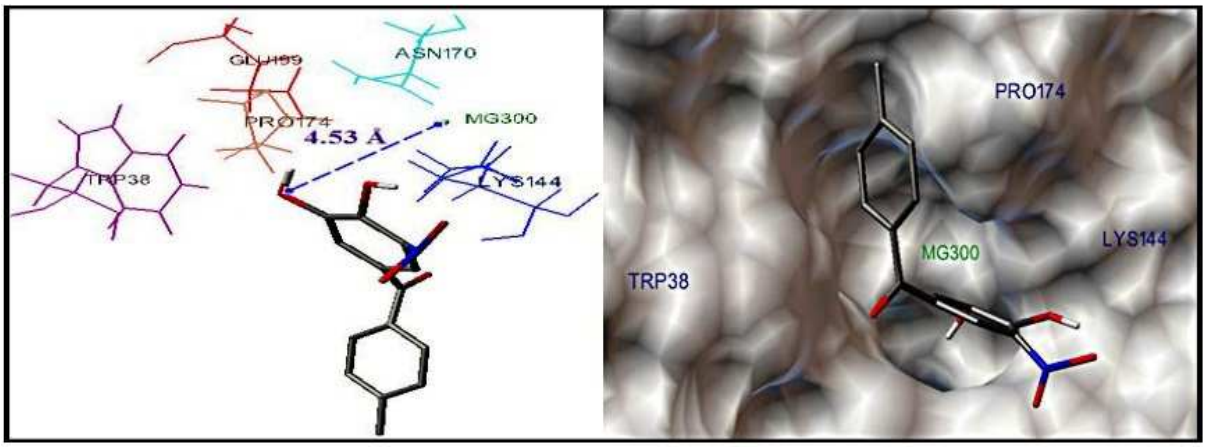

Fig. 9 Stereo and molecular surface view of the docking predicted pose and interaction of tolcapone within the active site of 1H1D

The compounds SB10 and SB33 both showed dipole-dipole interactions with the residue LYS 144. The results tabulated in Table 1, showed that 4 compounds among the 46 possesses better inhibition potential than the reference standard and many more were found in good agreement with the active site residues. The molecular surface view clearly demonstrates how well the active conformers of the respective compounds positioned them within the binding pocket. This study paved the way for further optimization of molecular skeleton considering the synthetic feasibility. According to the scoring energy all the compounds considered for the study has been categorized into potent inhibitors, Moderate inhibitors and Weak inhibitors (Figure 10-12).

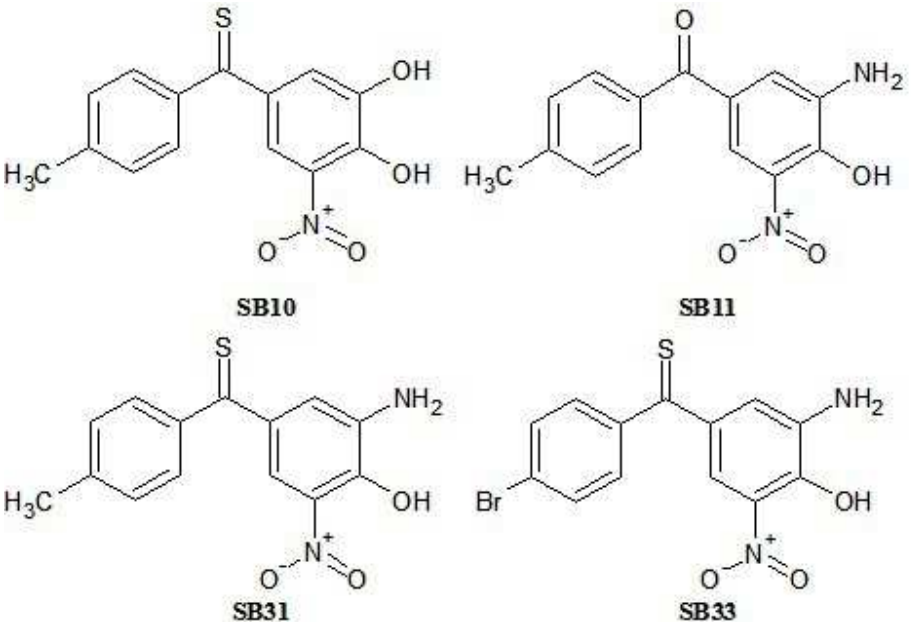

Fig. 10 Structure of Potent inhibitors

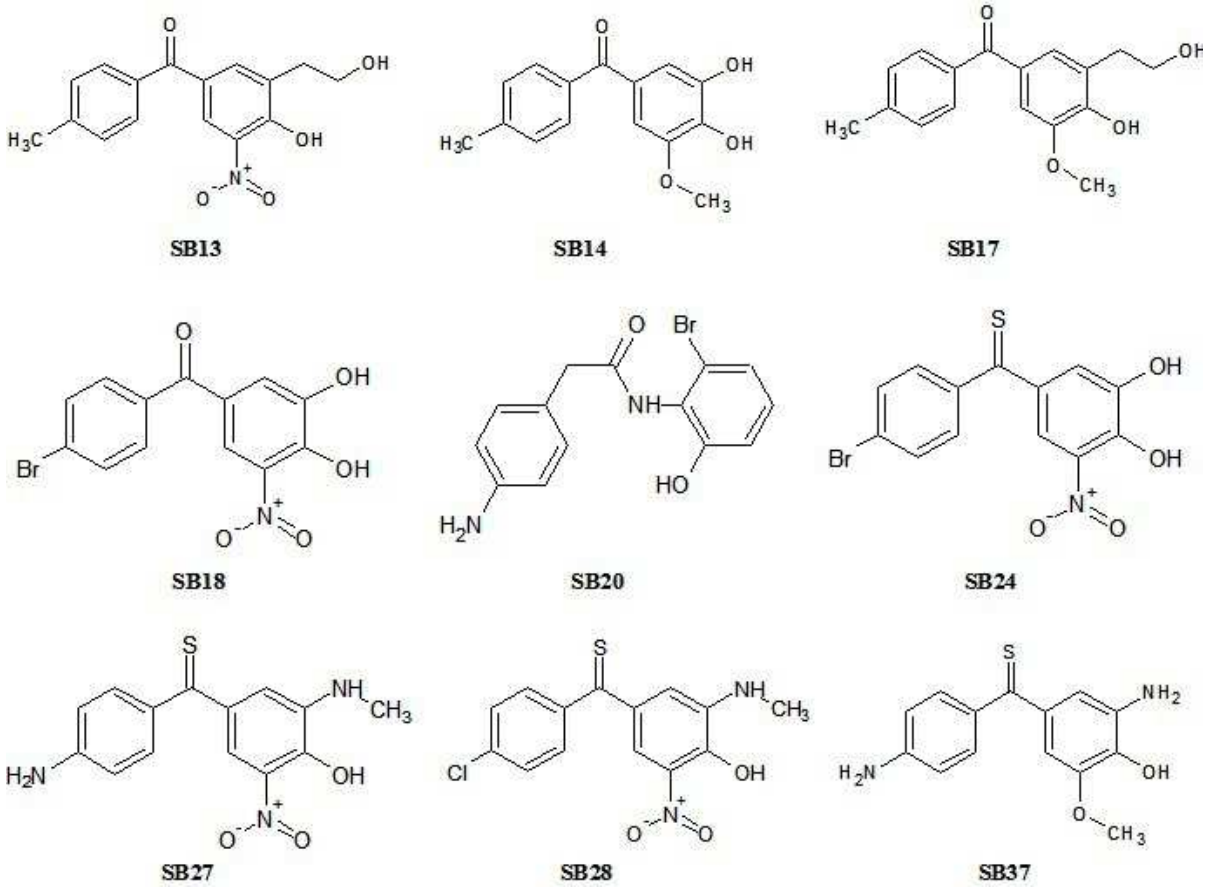

Fig. 11 Structure of Moderate inhibitors

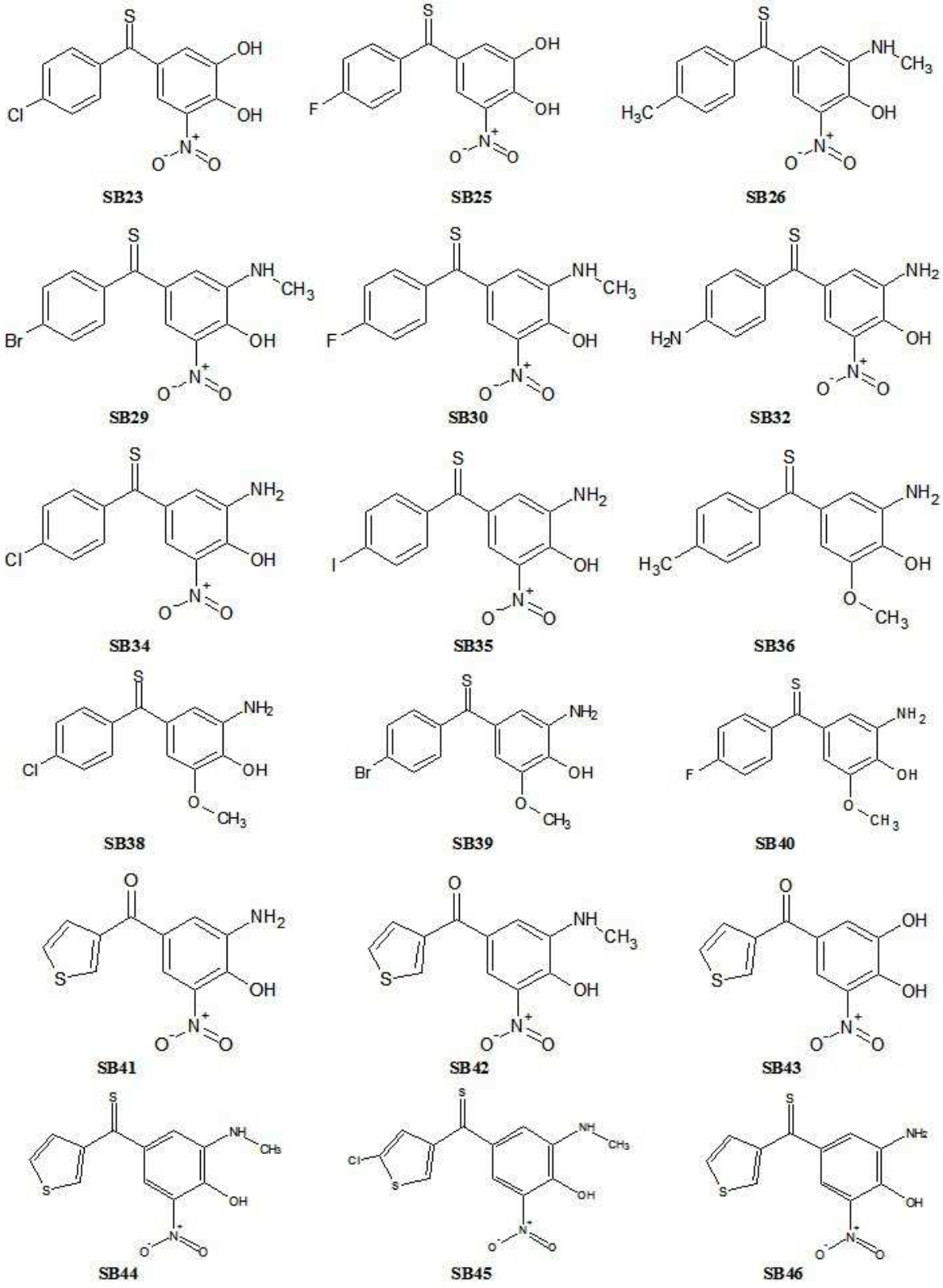

Fig. 12 Structure of Weak inhibitors

CONCLUSION

There is still significant space for extending the study, especially for the empirical binding free energy force field and KI prediction. The binding energy, inhibitory constant values, and binding interactions revealed from docking poses provide the clues for the design of novel compounds. These findings would be utilized for synthesizing and evaluating potent COMT inhibitors to be effectively introduced in the treatment of Parkinsonism.

Acknowledgement
The authors convey their sincere thanks to Principal and management, Gupta College of Technological Sciences, West Bengal, India.

REFERENCES

[1] PT Mannisto; S Kaakkola. *Pharmacol Sci*, **1989**, 10, 54.
[2] S Kaakkola; A Gordin; M Jarvinen; T Wikberg; E Schultz; E Nissinen; et al. *Clin Neuropharmacol*, **1990**, 13, 436.
[3] M Salminen; K Lundstrom; C Tilgmann; R Savolainen; N Kalkkinen; I Ulmanen. *Gene*, **1990**, 93, 241.
[4] B Bertocci; V Miggiano; MD Prada; Z Dembic; HW Lahm; P Malherbe. *Proc Natl Acad Sci USA*, **1991**, 88, 1416.
[5] K Lundstrom, M Salminen; A Jalanko; R Savolainen; I Ulmanen. *DNA Cell Biol*, **1991**, 10, 181.
[6] S Espinoza; F Manago; D Leo; TD Sotnikova; RR Gainetdinov. *CNS Neurol Disord Drug Targets*, **2012**, 11, 251.
[7] PT Mannisto; S Kaakkola. *Pharmacol Rev*, **1993**, 51, 593.
[8] PM Da; G Zurcher; A Napolitano. *Neurol*, **1995**, 45, 252.
[9] MJ Bonifacio, M Archer; ML Rodrigues; PM Matias; DA Learmonth; et al. *Mol Pharmacol* , **2002**, 62: 795,
[10] SA Allison; RJ Bacquet; JA McCammon. *Biopolymers*, **1988**, 27, 251.
[11] MP Bethune. *Antivir Res*, **2010**, 85, 75.
[12] RA Friesner; JL Banks; RB Murphy; TA Halgren; JJ Klicic; DT Mainz; et al. *J Med Chem*, **2004**, 47, 1739.
[13] Rarey M, Kramer B, Lengauer T, Klebe G. *J Mol Biol*, **1996**, 261, 470.
[14] DW Rodgers; SJ Gamblin; BA Harris; S Ray; JS Culp, et al. *Proc Nat Acad Sci USA*, **1995**, 92, 1222.
[15] AW Schuettelkopf, DMFV Aalten. *Acta Crystallographica*, **2004**, D60, *8*, 1355.
[16] MDL Rosa; HW Kim; E Gunic; C Jenket; U Boyle, et al. *Bioorg Med Chem Lett* **2006**, 16, 4444.
[17] RK Scott. *Biosilico*, **2004**, 2, 175.
[18] K Sharp; R Fine; B Honig. *Science*, **1987**, 236, 1460.
[19] FJ Solis; RJ-B Wets. *Math Oper Res*, **1981**, 6, 19.
[20] SJ Weiner; PA Kollman; DA Case; UC Singh; C Ghio; G Alagona; S Profeta; PA Weiner. *J Am Chem Soc*, **1984**, 106, 765.